Finite-Element Analysis of Jointed or Cracked Concrete Pavements

Amir M. Tabatabaie and Ernest J. Barenberg, Department of Civil Engineering, University of Illinois, Urbana-Champaign

A finite-element computer program called ILLI-SLAB and written in FORTRAN IV is described. The procedure is based on the classical theory of a medium-thick plate on a Winkler foundation and can be used for the analysis of concrete pavements that have joints or cracks or both. The program can include consideration of various types of load-transfer systems such as dowel bars, reinforcement steel, aggregate interlock, or keyways by treating the dowel bars and reinforcement steel as linear-elastic string elements and the aggregate interlock and keyways as linear-elastic spring elements. The model is also capable of handling the effects of stabilized bases or overlays on the stresses and deflections in concrete pavements and of traffic loadings on concrete shoulders that may or may not have tie bars, continuously reinforced concrete pavements, and slabs of varying thicknesses. The accuracy of the model for the prediction of stresses and deflections in concrete pavements has been verified by comparison with available theoretical solutions and the results of experimental studies.

The determination of stresses and deflections in concrete pavements that have joints or cracks or both has been a subject of major concern for several years. Because all of the analytical (closed-form) solutions are based on an infinitely large slab that has no, or at most, one discontinuity (1), they cannot be used for the analysis of jointed or cracked concrete slabs that have finite dimensions and load-transfer systems at the joints or cracks.

But the development of high-speed computers and the powerful finite-element method makes it possible to analyze concrete pavements in a more realistic manner. Various models have been developed for analyzing pavement systems by using finite-element modeling techniques. However, little has been done in modeling joints and cracks that have load-transfer systems.

Because of the three-dimensional geometry and the problem of stress concentration at the concrete pavement joints, the analysis should consider a three-dimensional approach. Although it is possible to formulate a three-dimensional finite-element model that would represent the whole system, the amount of discretization and the computer costs required for solution of the problem would be high and probably impractical.

Thus, a two-stage analysis of the jointed, concrete pavement system might provide a reasonable engineering approach: first, a two-dimensional analysis of the whole concrete pavement and then a three-dimensional analysis of a small section of the pavement at the joint that uses the results of the two-dimensional analysis in terms of the proper boundary condition. This paper describes the development of a two-dimensional finite-element model—which is called ILLI-SLAB and written in FORTRAN IV—for use in the first stage of analysis of a jointed or cracked concrete pavement.

The finite-element computer program presented here is based on the classical theory of a medium-thick plate on a Winkler foundation and is capable of evaluating the structural response of a concrete pavement system that has joints or cracks or both. The model, which provides several options, can be used to analyze the following types of problems:

1. Jointed concrete pavements that have load-transfer systems at the joints,
2. Jointed, reinforced concrete pavements that may or may not have cracks,
3. Continuously reinforced concrete pavements,
4. Concrete shoulders that may or may not have tie bars,
5. Concrete pavements that have a stabilized base or an overlay (by assuming either a perfect bond or no bond between two layers), and
6. Concrete slabs that have varying thicknesses and moduli of elasticity and subgrades that have varying moduli of support.

DESCRIPTION OF FINITE-ELEMENT MODEL

The assumptions about the concrete slab, stabilized base, overlay, subgrade, dowel bar, keyway, and aggregate interlock are summarized below:

1. The small-deformation theory of an elastic, homogeneous medium-thick plate can be used for the concrete slab, the stabilized base, and the overlay. Such a plate is thick enough to carry a transverse load by flexure, rather than in plane force (as would be the case for a thin membrane), and yet is not so thick that transverse shear deformation becomes important. It is assumed that lines that are normal to the middle surface in the undeformed plate will remain straight, unstretched, and normal to the middle surface in the deformed plate, that each lamina parallel to middle surface is in a state of plane stress, and that no axial or in-plane shear stress will develop because of loading.
2. The subgrade behaves like a Winkler foundation.
3. In case of a bonded stabilized base or overlay, there is full strain compatibility at the interface, and in the case of an unbonded base or overlay, the shear stresses at the interface are neglected.
4. The dowel bars at joints behave like a linear-elastic material and are located at the neutral axis of the slab.
5. When an aggregate interlock or a keyway is used as the load-transfer system, the load is transferred from one slab to an adjacent one by means of shear. However, when dowel bars are used as the load-transfer system, moment as well as shear may be transferred across the joints.

For modeling the concrete pavement slab, the rectangular plate element originally developed by Melosh (2) was used. The excellent performance of this element for modeling concrete pavements has been illustrated by several investigators (3, 4, 5). Figure 1a shows that at each node there are three displacement components—a vertical deflection (W) in the Z-direction, a rotation (θ_X) about the X-axis, and a rotation (θ_Y) about the Y-axis—and corresponding to these displacement components, there are three force components—a vertical force (P_W), a couple about the X-axis ($P_{\theta X}$), and a couple about the Y-axis ($P_{\theta Y}$) respectively. For each element, these forces and displacement can be related by matrix notation:

Figure 1. Finite-element model of pavement system.

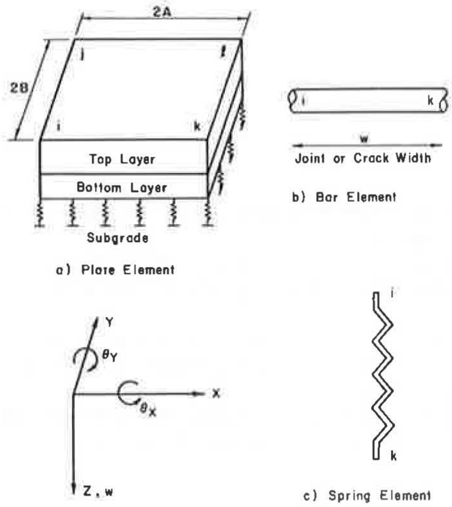

$$\{P\}_e = [K_{top} + K_{bottom} + K_{sub}]_e \{D\}_e \quad (1)$$

where $[K_{top}]_e$, $[K_{bottom}]_e$, and $[K_{sub}]_e$ are the stiffness matrices of the top layer, the bottom layer, and the subgrade respectively. $\{P\}_e$ is the force vector and $\{D\}_e$ the displacement vector of the slab element. For the case in which two layers (slab and stabilized base or slab and overlay) are bonded, an equivalent layer based on the transformed-section concept is used to determine the location of the neutral axis of the element. The following equations give the location of the neutral axis of a bonded two-layer system by using the first moment of the equivalent area of the transformed cross section.

$$\alpha = (1/2)(h_t + h_b)h_t/[h_t + (E_b/E_t)h_b] \quad (2)$$

$$\beta = (1/2)(h_t + h_b) - \alpha \quad (3)$$

where

α = distance from the middle surface of the bottom layer to the neutral axis,
β = distance from the middle surface of the top layer to the neutral axis,
H_t = thickness of the top layer,
h_b = thickness of the bottom layer,
E_b = modulus of elasticity of the top layer, and
E_b = modulus of elasticity of the bottom layer.

The bar element as shown in Figure 1b with 2 degrees of freedom/node is used to model the dowel bars at the joints. The two displacement components at each node are (a) a vertical displacement (W) in the Z-direction and (b) a rotation (θ_Y) about the Y-axis. Corresponding to these two displacement components, there are two forces: (a) a vertical force (P_W) and (b) a couple about the Y-axis ($P_{\theta Y}$). The force-displacement relation (including shear deformation) for each bar element can be written as

$$\{P\}_b = [K_{dowel}]_b \{D\}_b \quad (4)$$

where

$[K_{dowel}]_b$ = stiffness matrix of the dowel bars,
$\{P\}_b$ = force vector, and
$\{D\}_b$ = displacement vector of the bar element respectively.

The relative deformation of the dowel bar and surrounding concrete is represented as the stiffness of a vertical spring element (Figure 1c) that extends between the dowel bar and the surrounding concrete at the joint face.

If the moment transfer (if any) across a joint or crack where load transfer is achieved only by means of aggregate interlock or keyway is neglected, the spring element shown in Figure 1c with 1 degree of freedom/node can be used. The displacement component at each node is a vertical displacement (W) in the Z-direction, and the corresponding force component is a vertical force (P_W). The force-displacement relation for a spring element can be written as

$$\{P\}_s = [K_{Agg}]_s \{D\}_s \quad (5)$$

where

$[K_{Agg}]_s$ = stiffness matrix of the spring element,
$\{P\}_s$ = force vector, and
$\{D\}_s$ = displacement vector of the spring element respectively.

The overall structural stiffness matrix [K] is formulated by superimposing the effects of the individual element stiffnesses by using the topological (or the element-connecting) properties of the pavement system and used to solve the set of simultaneous equations that have the form

$$\{P\} = [K]\{D\} \quad (6)$$

where

$\{P\}$ = equivalent nodal forces for a uniformly distributed load over a rectangular section of the concrete slab and
$\{D\}$ = resultant nodal displacements for the whole system.

The generalized stresses are then calculated.

VERIFICATION OF THE FINITE-ELEMENT MODEL

To verify the accuracy of the finite-element computer program, it is necessary to compare the solutions found by using it with available theoretical solutions and the results of experimental studies. Westergaard's equations (6), Pickett's and Ray's influence charts (7), experimental studies at the AASHO test road (8), and tests conducted by Teller and Sutherland (9) have been used for this.

Figure 2 shows the comparison between the finite-element solutions and those found by using Westergaard's equations for a single load of 222 kN [50 000 lbf/in^2 (50 kips)] placed on one edge far away from any corner or in the interior of the slab far from any edges. (The finite-element computer program was developed for use with U.S. customary units only; therefore, values in Figures 2-6 and 8-13 are not given in SI units.) Because Westergaard's equations are based on an infinite slab, a large [7.6 m^2 (25 ft^2)] slab was used in the finite-element analysis. The loaded area in the Westergaard solution was assumed to be a circle having a 38-cm (15-in) diameter, and a square 38 cm on an edge was used in the finite-element analysis.

Figure 2. Comparison between finite-element solutions and those calculated by using Westergaard's equations.

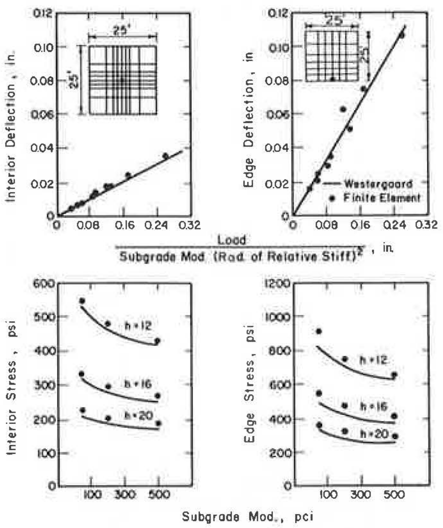

Figure 4. Comparison between edge stresses computed by using the finite-element program and those measured in AASHO Road Test.

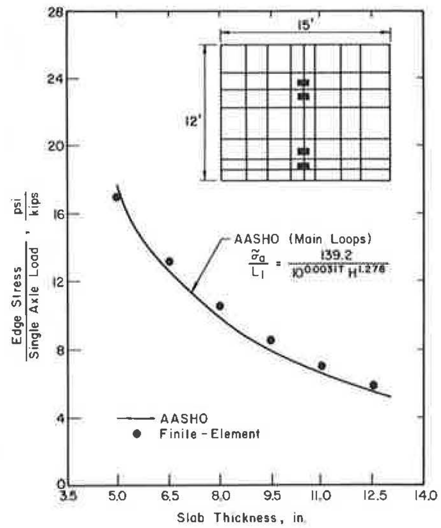

Figure 3. Comparison between finite-element solutions and those calculated by using influence charts.

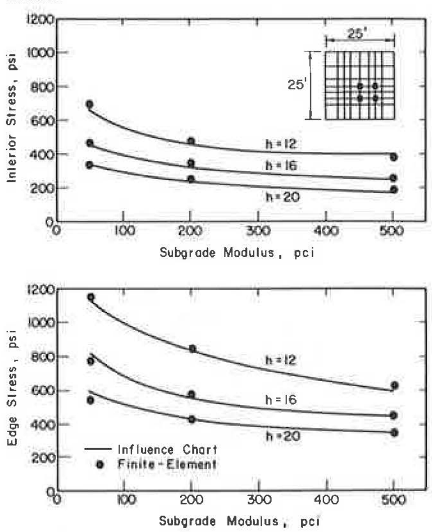

To verify the accuracy of the model for multiple loading, the influence charts developed by Pickett and Ray were used. Figure 3 shows the comparison between the finite-element and the influence-chart solutions for the main gear of a DC-10-10 aircraft that has a load of 978 kN (220 kips) placed at the edge or in the interior of the slab.

Further verification of the accuracy of the finite-element model was made by comparison with experimental results. The results of the strain measurements made in the AASHO Road Test (8) provide excellent data for such comparisons. The tests were conducted on the main traffic loops where the strain due to moving traffic 43 to 56 cm (17 to 22 in) from the edge was measured at the slab edge. The nonreinforced sections of the slabs were 4.6 m (15 ft) long, and the reinforced sections were 12.2 m (40 ft) long. The slab thicknesses ranged from 12.7 to 31.8 cm (5 to 12.5 in). The measured dynamic modulus of elasticity and Poisson's ratio of the concrete were found to be 43 GPa (6.250 000 lbf/in^2) and 0.28, respectively. The modulus of the subgrade reactions (k-values) on the subbase obtained by the plate-bearing tests varied from approximately 23 to 54 N/cm^3 (85 to 200 lbf/in^3) over all of the loops throughout the 2-year test period. An average value of 41 N/cm^3 (150 lbf/in^3) was used for the modulus of subgrade reaction in the finite-element analysis. Figure 4 shows the comparison between the finite-element solutions and the experimental results.

To verify the accuracy of the finite-element computer program for the prediction of stresses and deflections at concrete pavement joints that have various load-transfer systems, the results of the strain and deflection measurements made by Teller and Sutherland (9) were used. These tests were conducted on 10 full-sized concrete slabs, each 12.2 m (40 ft) long × 6.1 m (20 ft) wide. Four of the slabs had a uniform cross section, and the others had different, thickened-edge designs; their thicknesses ranged from 15.2 to 22.9 cm (6 to 9 in). Each slab was divided by a longitudinal and a transverse joint of a particular design, such as butt joints with different dowel spacings; joints that had a plane of weakness that had dowels; joints that had a plane of weakness, but no dowels; corrugated joints; and keyed joints that had triangular or trapezoidal tongues. The measured average modulus of elasticity of concrete and the modulus of subgrade reaction were found to be 37.9 GPa (5 500 000 lbf/in^2) and 54 N/cm^3, respectively. Figures 5 and 6 show the comparison between the finite-element solution and the experimental results.

These comparisons show that the finite-element solutions agree closely with both the theoretical and experimental results, which verifies the accuracy of the finite-element computer program developed in this study.

APPLICATION OF THE FINITE-ELEMENT MODEL

The finite-element procedure developed in this study is a powerful method for predicting stresses and deflections in jointed concrete pavements. To illustrate the application of the model, an example problem is presented. Assume that the effects of various types of joints on the stresses and deflections in a 30-cm (12-in) concrete slab

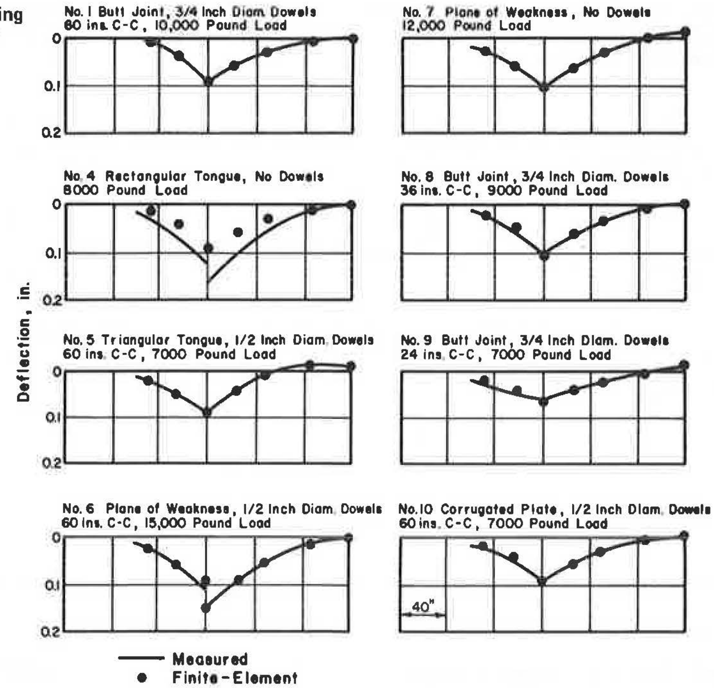

Figure 5. Comparison between slab deflections computed by using the finite-element program and those measured in the Bureau of Public Roads test.

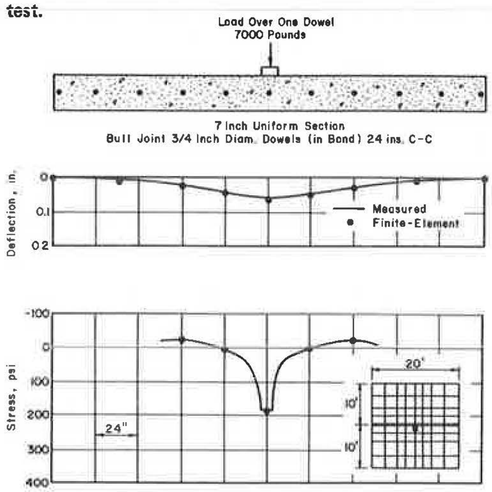

Figure 6. Comparison between joint deflections and stresses computed by using the finite-element program and those measured in the Bureau of Public Roads test.

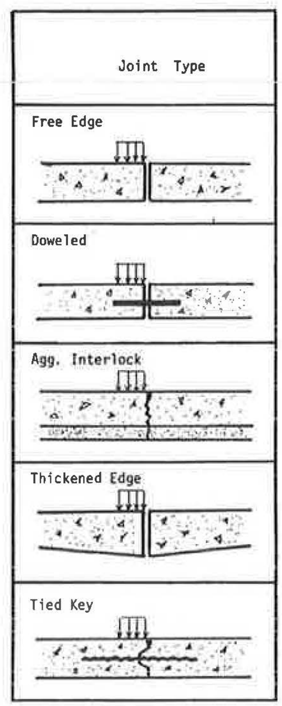

Figure 7. Different joint designs.

on a subgrade that has a k-value of 54 N/cm^3 are to be compared. A single load of 222 kN is applied uniformly over a 38-cm^2 area at the pavement joints, and the following joint designs are considered (see Figure 7).

1. A butt joint that does not have a load transfer system,
2. A doweled joint that has 32-mm (1.25-in) diameter dowels spaced at 38-cm center-to-center intervals and a 2.5-mm (0.1-in) joint-width opening (neglecting the effect of dowel-concrete interaction and dowel looseness),
3. A joint that has an aggregate-interlock system on a 10-cm (4-in) cement-stabilized base [Assume the spring stiffness for aggregate interlock (Agg) to be 34.45 MPa (5000 lbf/in^2), which is equivalent to 35 percent joint efficiency (Eff) (see Figure 8)],
4. A thickened-edge joint that has an edge thickness of 38 cm and no-load transfer system at the joint, and
5. A keyed joint that has tie bars [assume the spring stiffness (Agg) to be 68.9 GPa (1 000 000 lbf/in^2), which is equivalent to 100 percent Eff].

In the finite-element model, aggregate interlock is modeled as a series of vertical springs joining two adjacent slabs at the joint. The stiffness of these springs is related to the joint efficiency, which is a physical property of the joint and can be measured in the field. In this study, Eff is defined as the ability of the load-transfer system to transfer some of the applied load from the loaded slab to an adjacent slab and is determined as

$$\mathrm{Eff} = (\Delta_u/\Delta_L) \times 100 \qquad (7)$$

where Δ_L and Δ_u are the deflections of the loaded and unloaded slabs respectively. The relation between the spring stiffness and the joint efficiency is a function of slab and subgrade properties.

Figure 9 illustrates the finite-element mesh and the load configuration used in this example problem; the results of the maximum stresses and deflections for various joint designs are summarized below (1 MPa = 145 lbf/in² and 1 mm = 0.25 in).

Type of Joint	Max Edge Stress (MPa)	Max Edge Deflection (mm)
Free edge	5.25	1.3
Doweled	2.76	0.62
Agg interlock	3.44	0.86
Thickened edge	4.15	1.0
Tied key	2.73	0.64

These results show that the doweled and keyed joints (in this example problem) have larger reductions in maximum edge stress and deflection than the other joint designs. However, the final selection of the type of joint should also be based on the results of the three-dimensional analysis (to ensure that localized failure at the joint will not occur), performance, and construction cost.

Figure 10 shows a typical comparison of the finite-element solutions with the results of a conventional analysis of dowel reactions (distribution of shear forces along the joint) under edge loading that is based on Friberg's (10) analysis. In his study, Friberg observed that, according to Westergaard's (6) theoretical analysis, the maximum negative moment at a free slab edge under an edge loading occurs at a distance 1.8ℓ from the point of applied load, where ℓ is the radius of relative stiffness of the slab. Thus, it was assumed that the dowel bar immediately under the applied load carried its full capacity and that those on either side carried loads that decreased linearly to zero at a distance of 1.8ℓ from the central dowel. Because of the lack of useful analytical data, it was assumed that the distribution of transferred load was linear. However, as Figure 10 illustrates, the distribution of dowel shear forces among the dowel bars is not linear and only those dowels within distance ℓ from the central load are effective in transferring the load from the loaded slab to the adjacent one. Therefore, the maximum dowel shear force is higher than it was assumed by using the conventional dowel-shear analysis.

In concrete pavement design procedures, the effects of stabilized bases are usually included by using an equivalent subgrade modulus that is a function of the subgrade modulus and thickness of the base (11). However, in the finite-element method, a stabilized base was treated as a second rigid layer under the concrete slab. The elastic properties of the stabilized base and the condition of the bond between the slab and the base (perfect bond or no bond) are input to the finite-element program. This makes it possible to determine the stresses and deflections in the base as well as those in the slab directly from the program.

Figure 11 shows the effects of 10.2-, 15.2-, and 25.4-cm (4-, 6-, and 10-in) bonded-cement stabilized bases that have a modulus of elasticity of 6.89 GPa and a Poisson's ratio of 0.25 in reducing the maximum tensile edge stresses in 30.5-, 40.6-, and 50.8-cm (12-, 16-, and 20-in) thick concrete slabs. The maximum edge and interior stresses in slabs that do not have stabilized bases are also shown in this figure for comparison with the slabs on stabilized bases.

Further applications of the model are illustrated in Figures 12 and 13. Figure 12 shows the difference between the stress distribution along the joint of a concrete shoulder that is tied to the adjacent concrete slab and that along the joint of a shoulder that is not tied to the adjacent slab, both loaded by an 80-kN [18 000 lbf/in² (18-kip)] single-axle load placed with the inner tier of the centerline of the slab and the outer tier on the joint edge of the shoulder. In this case, the load-transfer system reduces the maximum stress in the concrete shoulder by approximately 50 percent. The concrete slab was assumed to be 20.3 cm (8 in) thick, 3.7 m (12 ft) wide, and 4.6 m (15 ft) long. The concrete shoulder was assumed to be 12.2 cm (6 in)

Figure 8. Relation between joint efficiency and spring stiffness.

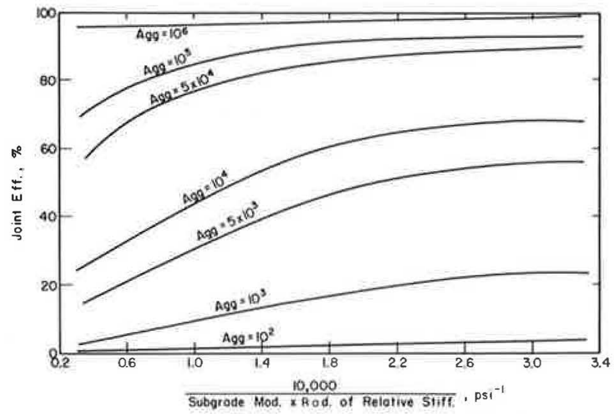

Figure 9. Typical finite-element mesh and load configuration (used for example problem).

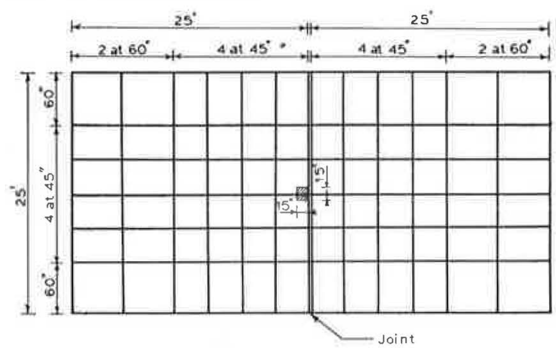

Figure 10. Distribution of dowel shear forces (transferred loads) by dowels along the joint.

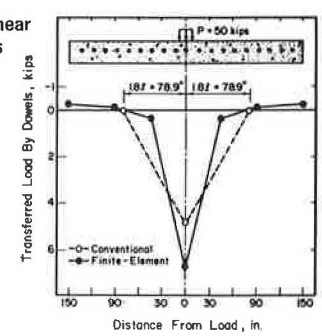

Figure 11. Effects of bonded stabilized bases in reducing maximum tensile edge stresses.

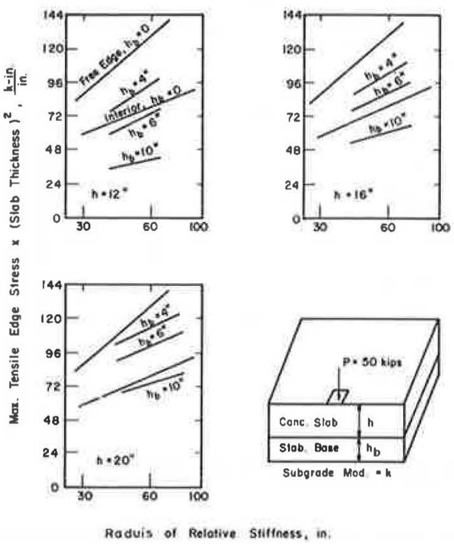

Figure 12. Stresses along the joint in concrete shoulder.

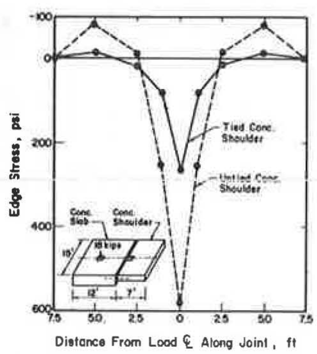

Figure 13. Effect of crack spacing on maximum stress in CRC pavement.

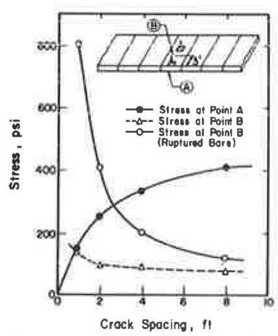

thick and 2.1 m (7 ft) wide. The modulus of elasticity of concrete and the subgrade modulus were assumed to be 34.5 GPa and 27 N/cm^3 (100 lbf/in^3) respectively.

Another application of the model—the determination of loading stresses only—in continuously reinforced concrete (CRC) pavements is shown in Figure 13. This figure shows the stresses in a 20.3-cm (8-in) thick CRC slab on a subgrade that has a k-value of 27 N/cm^3. An 80-KN single-axle load is applied at the edge of the slab midway between two cracks. The longitudinal reinforcing steel is assumed to have a diameter of 16 mm ($^5/_8$ in) and a center-to-center spacing of 12.2 cm. This figure shows that, as the average crack spacing in the CRC pavement is reduced, the edge stress at the bottom of the slab at point A is also reduced and the stress at point B, which is about 91 cm (3 ft) from the slab edge and in transverse direction, is increased. The rate of this increase of the slab stress at point B is highly affected by the conditions of the longitudinal steel and the aggregate interlock at the cracks. When the cracks are tight, the increase in the stress at point B is small because the crack spacing is reduced. However, when the cracks are opened up and the steel bars are ruptured, the increase in the stress at point B is large and easily can cause longitudinal cracks and punchouts.

SUMMARY

A finite-element program based on the classical theory of a medium-thick plate on a Winkler foundation was developed for analysis of jointed or cracked concrete pavements. The model is capable of evaluating the effects of various load-transfer systems, such as dowel bars, aggregate interlock, and keyways on the stresses and deflections in concrete pavements. Furthermore, the model, which provides several options, can be used for the analysis of a number of problems such as jointed, reinforced concrete pavements that are cracked, continuously reinforced concrete pavements, concrete slabs that have stabilized bases or overlays, concrete shoulders, and slabs of varying thicknesses.

The model was verified by comparing the finite-element solutions with available theoretical solutions and the results of experimental studies. Several example problems were solved to illustrate its capabilities.

ACKNOWLEDGMENTS

This study was conducted by members of the staff of the Department of Civil Engineering, University of Illinois at Urbana-Champaign. The project was sponsored by the Federal Aviation Administration and the Federal Highway Administration, U.S. Department of Transportation. The opinions, findings, and conclusions expressed are ours and not necessarily those of the sponsoring agencies.

REFERENCES

1. H. P. Niu and G. Pickett. The Effect of Degree of Continuity Across a Void or Crack on Performance of Concrete Pavements. HRB, Highway Research Record 291, 1969, pp. 186-193.
2. R. J. Melosh. Basis for Derivation of Matrices for the Direct Stiffness Method. Journal of the AIAA, Vol. 1, No. 7, 1963, pp. 1631-1637.
3. Y. H. Huang and S. T. Wang. Finite-Element Analysis of Concrete Slabs and Its Implications for Rigid Pavement Design. HRB, Highway Research Record 466, 1973, pp. 55-69.
4. A. C. Eberhardt. Aircraft-Pavement Interaction Studies—Phase 1: A Finite-Element Model of a Jointed Concrete Pavement on a Nonlinear Viscous Subgrade. U.S. Army Corps of Engineers Computer-Based Eucation Research Laboratory, Champaign, IL, Rept. S-19, 1973.
5. Y. H. Huang. Finite-Element Analysis of Slabs on Elastic Solids. Transportation Engineering Journal, Proc., ASCE, Vol. 100, No. TE2, May 1974, pp. 403-416.
6. H. M. Westergaard. Computation of Stresses in Concrete Roads. Proc., HRB, Vol. 6, 1926, pp. 25-35.
7. G. Pickett and G. K. Ray. Influence Charts for Concrete Pavements. Trans., ASCE, Vol. 116, 1951, pp. 49-73.
8. The AASHO Road Test: Report 5—Pavement Re-

search. HRB, Special Rept. 61E, 1962.

9. L. W. Teller and E. C. Southerland. The Structural Design of Concrete Pavements. Public Roads, Vol. 16, Nos. 8, 9, and 10 (Oct., Nov., and Dec. 1935); Vol. 17, Nos. 7 and 8 (Sept. and Oct. 1936); and Vol. 23, No. 8 (April-June 1943).
10. B. F. Friberg. Design of Dowels in Transverse Joints of Concrete Pavements. Trans., ASCE, Vol. 105, 1940, pp. 1809-1828.
11. Thickness Design for Concrete Pavements. Concrete Information, PCI, 1966.

Discussion

Y. H. Huang, University of Kentucky
Y. T. Chou, U.S. Army Engineer Waterways Experiment Station, Vicksburg, Mississippi

The authors have presented a very powerful method for analyzing joints in concrete pavements. In a previous paper (12), a finite-element method was developed for the analysis of jointed concrete pavements by specifying the efficiency of load transfer across the joints. Because the efficiency of load transfer depends not only on the type of joints but also on many other factors, such as the magnitude and location of the applied loads, the pavement thickness, and the subgrade modulus, it is quite difficult to ascertain what efficiency should be used in the actual analysis. The use of spring elements to model aggregate interlock or keyways and bar elements to model doweled joints will solve the problem deterministically. The authors are to be complimented for their effort in this direction.

The discussion we would like to present here is whether it is logical to model dowels or reinforcement steel as bar elements. Figure 14a is a schematic diagram of the bar element, as presented by the authors. This diagram is misleading because the width of the joint or crack is generally much smaller than the bar diameter, and the element should be drawn as shown in Figure 14b. It is apparent that a bar such as that shown in Figure 14b serves merely as a key to transmit shear. This agrees with the current concept that load is transferred across a joint principally by shear. Ball and Childs (13) have reported that some moment may be transferred through tie joints that remain closed, but moment transfer across joints with visible openings is negligible.

It is well known that the amount of stress reduction at a joint is governed by the difference in deflection between the two slabs along the joint. This difference depends primarily on the dowel-concrete interaction. Neglecting the deformation of the concrete surrounding the dowel bar will make the bar appear much more effective than it actually is. The first two examples presented by the authors indicate that the dowel bar reduces the edge stress from 5.25 to 2.76 MPa, which is a stress reduction of 48 percent. Our results show, however, that because of the large effect of the dowel-concrete reaction, the actual stress reduction is only 22 percent. Our data show that the maximum edge deflection is 0.66 mm (0.0259 in) on the loaded slab and 0.49 mm (0.0193 in) on the unloaded slab, which is a difference in deflection of 0.17 mm (0.0066 in) of which 0.16 mm (0.0062 in) is contributed by the dowel-concrete interaction and only 0.01 mm (0.0004 in) by the shear deformation of the dowel bar. The greater effect of the dowel-concrete interaction is quite apparent. If the dowel-concrete interaction is neglected, the shear deformation of the dowel is increased to 0.02 mm (0.0007 in) because of the increase in shear force, and the stress reduction becomes 43 percent.

The percentage of the stress reduction that should be ascribed to the dowel bars can be computed by two different methods. The first requires the solution of two separate problems, one with the loading adjacent to a free edge and the other with it adjacent to a doweled joint, and can be determined as

$$\text{Stress reduction} = 100\,[1 - (\text{stress at doweled joint} \div \text{stress at free edge})] \tag{8}$$

The second requires the solution of only one problem, i.e., the determination of the stresses on both sides of a doweled joint and is determined as

$$\text{Stress reduction} = 100\,\{1 - [\text{stress on loaded slab} \div (\text{stress on loaded slab} + \text{stress on unloaded slab})]\} \tag{9}$$

It was found that both equations give almost the same result because the sum of the stresses on both sides of the joint is nearly a constant and equal to the stress at the free edge.

The extreme effectiveness of the dowel bar, as reported by the authors, does not seem to agree with the experimental evidence. In the design and evaluation of rigid pavements, the U.S. Army Corps of Engineers assumes a minimum stress reduction of 25 percent. The results of a series of full-scale, static loading tests conducted at eight U.S. Air Force bases throughout the continental United States in 1959 indicated that the average value of stress reduction for doweled construction joints was about 28 percent (14). The same finding was also obtained in small-scale model tests (15).

Our method for the analysis of doweled joints is quite different from the authors'. First, we consider that dowel bars can only transmit shear. Second, we include the dowel-concrete interaction by assuming that the dowel bar acts as a beam and the concrete as an

Figure 14. Modeling of dowels.

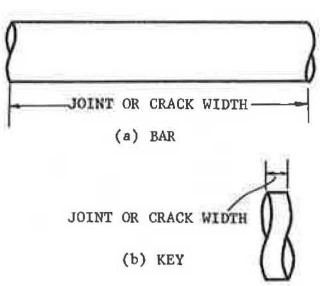

Figure 15. Difference in deflection between two slabs.

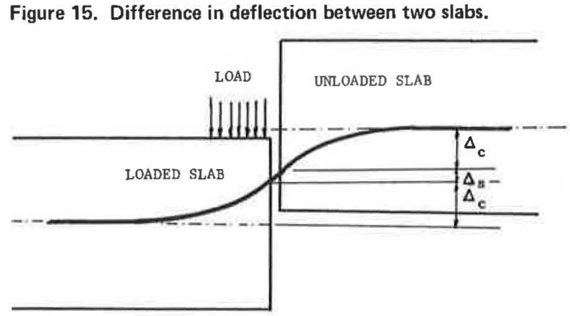

elastic foundation (16) (see Figure 15). The difference in deflection between the two slabs at the joint is equal to $\Delta_s + 2\Delta_c$, where Δ_s = shear deformation of the dowel bar and Δ_c = deformation of concrete due to shear force on the dowel bar. The vertical shear force applied at each node along the joint can be determined by a method of successive approximations as follows:

1. Considering the left (or loaded) slab only and disregarding the right slab, determine the displacements of the left slab due to the applied load;
2. Determine the displacements of the right (or unloaded) slab by setting the vertical deflections of the right slab along the joint equal to those of the left;
3. Determine the vertical nodal (or shear) force at the joint due to the displacements of the right slab and compute the difference in deflection between the two slabs, which is equal to $\Delta_s + 2\Delta_c$;
4. Determine the displacements of the left slab due to the combined effects of the applied load and the vertical nodal forces along the joint due to the right slab;
5. Determine the displacements of the right slab by setting the deflections along the joint equal to the deflections of the left minus the difference in deflection $(\Delta_s + 2\Delta_c)$; and
6. Repeat steps 3 to 5 until the vertical nodal forces along the joint converge to a specified tolerance.

To verify the validity of the method, the finite-element solutions were compared with the field tests conducted at four U.S. Air Force bases (14). In these tests, strains parallel to the longitudinal construction joint were measured on both sides of the joint, one on the loaded slab and the other on the unloaded slab. Because there is no stress normal to the joint, the stress along the joint is directly proportional to the strain. Consequently, the percentage of stress reduction can be computed from Equation 9 simply by replacing the stress with the strain. The aircraft used for the test was a B-47 that had a forward gear load of 420 kN (94 500 lbf) distributed over two wheels 94 cm (37 in) apart.

A comparison between the stress reductions calculated by the theoretical method and those found experimentally is given in Table 1. The subgrade modulus at each location was determined from field tests and is reported elsewhere (14). It can be seen that the theoretical solutions agree well with the experimental measurements. The theoretical solutions are based on a modulus of dowel support of 407 GN/m^3 (1 500 000 lbf/in^3). Values reported for the modulus of dowel support, which varies with the amount of looseness between the dowel and the concrete, range from 81 GN/m^3 (300 000 lbf/in^3) to 2450 GN/m^3 (9 000 000 lbf/in^3) (17). If the low value is assumed for the site at Lockbourne and the high value for that at Lincoln, the percentages of load transfer are 23.4 and 34.9 respectively, which agree closely with the measured values of 21.1 and 36.8.

Table 1. Comparison of theoretically calculated and experimentally measured stress reductions.

Location	Pavement Thickness (cm)	Subgrade Modulus (MN/m^3)	Dowel Diameter (cm)	Dowel Spacing (cm)	Stress Reduction (%) Experimental	Stress Reduction (%) Theoretical
Lockbourne Air Force Base, Ohio	30.5	20.2	2.5	38.1	21.1	26.3
Lincoln Air Force Base, Nebraska	53.3	17.6	3.8	25.4	36.8	29.6
Hunter Air Force Base, Georgia	45.7	47.5	3.8	45.7	27.1	24.6
McCoy Air Force Base, Florida	45.7	61.2	3.8	45.7	23.1	23.6

Note: 1 cm = 0.4 in and 1 MN/m^3 = 3.78 lbf/in^3.

REFERENCES

12. Y. H. Huang and S. T. Wang. Finite-Element Analysis of Concrete Slabs and Its Implications for Rigid Pavement Design. HRB, Highway Research Record 466, 1973, pp. 55-79.
13. C. G. Ball and L. D. Childs. Test of Joints for Concrete Pavements. PCA, Research and Development Bulletin RD026.01P, 1975.
14. Field Tests of Doweled-Joint Performance. U.S. Army Engineer Ohio River Division Laboratories, Cincinnati, OH, Final Rept., Nov., 1959.
15. Small-Scale Model Study of Doweled Joints in Rigid Pavement for Military Airfields. U.S. Army Engineer Ohio River Division Laboratories, Cincinnati, OH, Unpublished Rept., 1959.
16. E. J. Yoder and M. W. Witczak. Principles of Pavement Design. Wiley, New York, 1975, pp. 98-99.
17. E. A. Finney. Design of Dowels in Transverse Joints of Concrete Pavements. Journal of the American Concrete Institute, Proc. Vol. 53, No. 1, July 1956.

Authors' Closure

We thank the discussants for their review of the paper. They have presented some valuable suggestions, and we think that it is appropriate to give specific responses to their comments.

On their comment as to whether it is logical to model dowels as bar elements, we think it is logical and also realistic to model them as such because this allows the model to become a general purpose model that can be used for the analysis of doweled joints in which the joint openings are small, such as for contraction joints, as well as for the analysis of doweled joints in which the openings are large. However, modeling dowels as keys, as was suggested by the discussants, would restrict the model to the analysis of systems in which the joint openings are small in comparison with the dowel diameter.

We fully agree with the discussants' comment regarding the importance of considering dowel-concrete interaction on the doweled joint stresses, which was neglected for convenience for the doweled joint system shown in our paper. As a matter of fact, dowel-concrete interaction is an input to the finite-element program in terms of the stiffness of a vertical spring between the dowel bar and the surrounding concrete at the joint face. The force-displacement relation for this spring element can be written as

$$F = K_{DCI}\,\Delta \qquad (10)$$

where

K_{DCI} = stiffness of the spring element representing the dowel-concrete interaction,
F = shear force on the dowel bar, and
Δ = relative deformation of the dowel bar with respect to the surrounding concrete at the joint face.

But the important question is how to determine a realistic dowel-concrete interaction (K_{DCI}). It is our judgment that the manner that the discussants have suggested is not valid because of the three-dimensional nature of the problem and also because of the problem of dowel looseness.

The discussants have suggested the use of a conventional dowel analysis based on the principles first given by Timoshenko (18), where a bar encased in concrete was modeled as a semi-infinite beam uniformly supported on a Winkler-type foundation. The rate at which the concrete reacts against deflection of the dowel bar is referred to as modulus of dowel support (K), which appears in the force-displacement relation. The modulus of dowel support in this analysis is analogous to the modulus of subgrade support in the analysis of a concrete slab on a Winkler-type foundation.

A major problem in the use of this analysis is the selection of the appropriate modulus of dowel support. The results given below (19) show a wide range of values (1 GN/m^3 = 3860 lbf/in^3).

Modulus of Dowel Reactions (GN/m^3)	Source	Method	Date
81-408	Grinter	Estimation	
Max 680	Friberg	Tests on embedded dowels	1938
193-308	Michigan State Highway Department	Load-deflection tests	1947
212-1605	Michigan State Highway Department	Tests on embedded dowels	1947
242-2260	Marcus	Dowels with uniform bearing pressure	
667	Loe	Load-deflection tests	1952
245-2340	Michigan State Highway Department	Tests on embedded dowels	1954

This range in K-values is probably due in large measure to looseness between the dowel and the concrete. The effect of the modulus of the dowel reaction on the edge stresses and deflections of the doweled joint (example problem 1 above) is shown below (1 MPa = 145 lbf/in^2 and 1 mm = 0.04 in).

K (GN/m^3)	Max Edge Stress (MPa)	Max Edge Deflection (mm)
81	4.28	0.81
408	4.68	0.71
2340	3.14	0.66

It can be seen that, depending on the values used for the modulus of the dowel reaction, edge stresses at the doweled joint can vary considerably.

Dowel looseness consists of two parts, initial looseness and looseness caused by repetitive loads. In a series of laboratory tests conducted by Teller and Cashell (20), it was found that the dowel looseness can vary about 0.05 to 0.10 mm (0.002 to 0.004 in) initially and increases when the doweled joints are subjected to heavy loads or many applications of lighter loads (13, 14, 20). The effect of dowel looseness on the maximum edge stresses and deflections of the doweled joint (example problem 1 above) is shown below.

Dowel Looseness (mm)	Max Edge Stress (MPa)	Max Edge Deflection (mm)
0.025	3.10	0.66
0.075	3.65	0.71
0.125	4.00	0.66

It can be seen that, depending on the amount of dowel looseness, edge stresses in the slab can vary considerably.

The conventional dowel analysis suggested by the discussants is based on the assumption of full dowel support and is not capable of handling the problem of dowel looseness. The effect of dowel looseness in jointed slab analysis is analogous to the effect of loss of foundation support in the analysis of a concrete slab, and for a realistic analysis, some information about the magnitude and shape of the gaps is needed. The discussants have suggested the use of an arbitrarily reduced or increased value for the modulus of dowel support, to include the effect of dowel looseness, but this approach does not appear logical to us because no correlation has been established between dowel looseness and the measured values of K.

In reality, the interaction between a loaded dowel and the surrounding concrete is in a three-dimensional state of stress (21) and this interaction depends on dimensions and elastic properties of the dowel bar and concrete slab, plus any looseness there might be between the dowel bar and the surrounding concrete. This makes the conventional dowel-concrete-interaction approach applicable. This was the reason, as noted in the introduction of the paper, that a three-dimensional analysis of the concrete slab near the joint and around a dowel was used in conjunction with the two-dimensional analysis of the jointed slab to establish a realistic dowel-concrete interaction.

A complete analysis that includes the results of a three-dimensional model (22) of dowel-concrete interaction analysis is being prepared and will be given in another paper. In this paper, actual elastic properties and the dimensions of the concrete slab and dowel bar, rather than the modulus of dowel support, are used to establish a dowel-concrete interaction (K_{DCI}) that can be used as an input to the finite-element program for jointed-slab analysis.

REFERENCES

18. S. Timoshenko and J. M. Lessels. Applied Elasticity. Westinghouse Technical Night School Press, Pittsburgh, PA, 1925.
19. E. A. Finney. Structural Design Considerations for Pavement Joints. Journal of the American Concrete Institute, Vol. 53, No. 1, July 1956, pp. 1-28.
20. L. W. Teller and H. D. Cashell. Performance of Dowels Under Repetitive Loading. Public Roads, Vol. 30, No. 1, April 1958.
21. H. Marcus. Load-Carrying Capacity of Dowels at Transverse Pavement Joints. Journal of the American Concrete Institute (ACI, Proc. Vol. 48), Vol. 23, No. 2, Oct. 1951, pp. 169-184.
22. B. M. Irons. Engineering Application of Numerical Integration in Stiffness Methods. Journal of the American Institute of Aeronautics and Astronautics, Vol. 4, No. 11, 1966, pp. 2035-2037.

Publication of this paper sponsored by Committee on Rigid Pavement Design.